Lázaro, M. (2019). Approximate critical curves in exponentially damped nonviscous systems. Mechanical Systems and Signal Processing. 122:720-736. https://doi.org/10.1016/j.ymssp.2018.12.044

Approximate critical curves in exponentially damped nonviscous systems

M. Lázaro[a,*]

[a]*Department of Continuum Mechanics and Theory of Structures*
Universitat Politècnica de València 46022 Valencia, Spain

Abstract

In this paper a new approximate numerical method to obtain critical curves in exponentially damped nonviscous systems is proposed. The assumed viscoelastic forces depend on the past history of the velocity response via convolution integrals over exponential kernel functions. Critical surfaces are manifolds in the multidimensional domain defined by the damping parameters, depicting thresholds between the induced oscillatory and non-oscillatory motion. If these surfaces are formed by two parameters, then they are named critical curves. The available method in the literature to construct these curves involves the analytical manipulation of the transcendental matrix determinant, something that can become highly inefficient for large systems. In this paper, it is proved that approximate critical curves can be constructed eliminating the Laplace parameter from two eigenvalue problems: the original one controlled by the dynamical stiffness matrix and another one defined by its derivative respect to the Laplace parameter. The theoretical background of the approach is derived with help of the implicit function theorem. It turns out that the so-found approximate overdamped regions are enclosed by a set of critical curves, which can be derived in parametric form. The proposed method is validated through two numerical examples involving multiple degrees of freedom.

Keywords:
nonviscous damping, critical damping, exponential damping, overdamped region, critical curves, approximate method

1. Introduction

In this paper, nonviscously damped vibrating linear systems are considered. Nonviscous damping models describe the dynamical behavior of viscoelastic materials, also known as time-dependent materials. The induced dissipative forces depend on the past history of the velocity response via convolution integrals over hereditary kernel functions. Let $\mathbf{u}(t) \in \mathbb{R}^n$ denote the column vector with the degrees of freedom (dof) of the system, then the governing equations of motion can be written in integro-differential form as [1]

$$\mathbf{M}\ddot{\mathbf{u}} + \int_{-\infty}^{t} \boldsymbol{\mathcal{G}}(t-\tau)\,\dot{\mathbf{u}}\,\mathrm{d}\tau + \mathbf{K}\mathbf{u} = \mathbf{f}(t) \tag{1}$$

where $\mathbf{M}, \mathbf{K} \in \mathbb{R}^{n\times n}$ are the mass and stiffness matrices assumed to be positive definite and positive semidefinite, respectively; $\boldsymbol{\mathcal{G}}(t) \in \mathbb{R}^{n\times n}$ is the damping matrix in time domain, assumed symmetric. This matrix contains damping models which satisfy the necessary conditions of Golla and Hughes [2] to induce a strictly dissipative motion. The widespread used viscous model can be considered just as a particular case of Eq. (1) with $\boldsymbol{\mathcal{G}}(t) \equiv \mathbf{C}\,\delta(t)$, where $\mathbf{C}$ is the viscous damping matrix and $\delta(t)$ the Dirac's delta function. The motion equations yield then

$$\mathbf{M}\ddot{\mathbf{u}} + \mathbf{C}\dot{\mathbf{u}} + \mathbf{K}\mathbf{u} = \mathbf{f}(t) \tag{2}$$

*Corresponding author. Tel +34 963877000 (Ext. 76732). Fax +34 963877189
Email address: malana@mes.upv.es (M. Lázaro)

Checking exponential-like solutions $\mathbf{u}(t) = \boldsymbol{u}\, e^{st}$ in Eq. (1) yields to the nonlinear eigenvalue problem associated to viscoelastic vibrating structures

$$\left[s^2\mathbf{M} + s\mathbf{G}(s) + \mathbf{K}\right] \boldsymbol{u} \equiv \mathbf{D}(s)\, \boldsymbol{u} = \mathbf{0} \tag{3}$$

where $\mathbf{G}(s) = \mathcal{L}\{\boldsymbol{\mathcal{G}}(t)\} \in \mathbb{C}^{n\times n}$ is the damping matrix in the Laplace domain, $\mathbf{D}(s)$ is the dynamical stiffness matrix or transcendental matrix and s is the Laplace parameter. The set of eigenvalues are the roots of the characteristic equation

$$\det\left[\mathbf{D}(s)\right] = 0 \tag{4}$$

The oscillatory nature of these eigenvalues depends on the dissipation level induced by the damping model, mathematically represented by $\mathbf{G}(s)$. Although some additional details on this matrix will be established later, for the time being it is just necessary to know that in general $\mathbf{G}(s)$ depends not only on the Laplace variable s, but also on certain number of parameters. These parameters someway depict the damping level and the viscoelasticity of the system. Viscoelasticity (or non-viscousity) deals with the frequency dependence of the damping model; hence small variations lead the system to a viscous-like behavior. On the other hand, damping level affects directly on the dissipative capacity of the system and it can be read as how far is the system from the undamped state. Lightly damped systems present in general $2n + p$ eigenvalues, namely n conjugate-complex pairs representing modes with oscillatory nature and p real eigenvalues without oscillatory nature, associated to hereditary exponential kernels [1, 3, 4]. For certain combination of the damping parameters, some (or maybe all) conjugate-complex pair could drop on the real axis, changing the nature of the motion of some mode from oscillatory to non-oscillatory. In the domain of the damping parameters, those thresholds between induced oscillatory and non-oscillatory motion are called critical damping surfaces or manifolds. Beskos and Boley [5] for viscous systems and recently Lázaro [6] for those nonviscous ones, established that critical damping manifolds arise from eliminating the Laplace parameter s from the two following equations

$$\det\left[\mathbf{D}(s)\right] = 0 \quad , \qquad \frac{\partial}{\partial s}\det\left[\mathbf{D}(s)\right] = 0 \tag{5}$$

Critical damping in viscous systems has been extensively investigated in the bibliography. Duffin [7] analyzed overdamping in linear systems in terms of quadratic forms of the coefficient matrices. Nicholson [8] deduced eigenvalue bounds deriving sufficient condition for subcritical damping. Müller [9] gave mathematical characterizations of underdamped system similarly to Duffin's work but deriving sufficient condition involving the definiteness of the system matrices. Inman and Andry [10] proposed sufficient conditions for underdamped, overdamped and critically damped motions in terms of the definiteness of the system matrices. Barkwell and Lancaster [11] pointed out some defects in the Inman and Andry criterion of ref. [10] providing some explanations justifying why this criterion has been frequently used to check criticality in damped systems. Barkwell and Lancaster [11] derived conditions for overdamping in gyroscopic linear sytems. Bhaskar [12] corrected the Inman and Andry's criterion giving more general conditions for complete overcritical damping.

In reference to non–viscous linear systems, Muravyov and Hutton [13] and Adhikari [14] studied the conditions for critical damping of single dof systems with Biot's damping model based on one exponential kernel. Instead of using Eqs. (5), an exhaustive analysis of the roots nature of the resulting third order characteristic polynomial is carried out in ref. [14]. Müller [15] addressed the nature of the eigensolutions of a single dof Zener 3–parameter non–viscous model. Muravyov [16] derived closed-form solutions for forced nonviscoulsy damped beams studying the conditions for overdamping or underdamping time response. Lázaro [6] extended for nonviscous systems the Beskos and Boley's approach of ref. [5], determining critical curves for single dof systems with two exponential kernels and also for multiple dof systems. However, the methods in refs. [5, 6] to find critical surfaces for viscous and non–viscous systems are somehow limited by the size of the system since equations are expressed in terms of the determinant of the system and its derivative. The determination of closed–form expressions for these equations becomes computationally inefficient for large systems. Papargyri-Beskou and Beskos [17] improved its approach for viscous systems proving that the critical surfaces of viscously damped systems with damping matrix $\mathbf{C}$ can be approximated

by those implicitly defined by the following expressions

$$\det\left[\omega_j^2\mathbf{M}-\omega_j\mathbf{C}+\mathbf{K}\right]=0 \quad , \; 1\leq j\leq n \tag{6}$$

where $\omega_j>0$ is the jth natural frequency of the associated undamped problem.

The challenge of this paper is to extend the results of Papargyri-Beskou and Beskos [17] for nonviscously damped systems. Firstly, the conditions to obtain approximate critical surfaces for nonviscous damping are deduced using the implicit function theorem. Mathematically, these conditions are equivalent to eliminate the Laplace parameter s from the equations $\det\left[\mathbf{D}(s)\right]=0$ and $\det\left[\mathbf{D}'(s)\right]=0$. Secondly, approximate critical curves are derived for exponentially damped systems whose matrix can be written in the form $\boldsymbol{\mathcal{G}}(t)=\mu\, e^{-\mu t}\,\mathbf{C}$. The total available number of critical curves with this method is proved to be equal to $n\times\mathrm{rank}\,(\mathbf{C})$. The overdamped region arises as the envelope of the regions enclosed by the found critical curves. The proposed approach is strongly related to the critical curves of a single degree of freedom, hence this latter case is studied in depth. In addition, the method has been validated for two multiple dof systems: an array of 4-dof spring-mass system and a 36-dof continuous beam with discrete nonviscous constraints.

2. Approximate determination of critical damping

Papargyri-Beskou and Beskos [17] proved that critical damping surfaces of viscously damped systems can be approximated as manifolds (written en terms of the damping coefficients), as a result of the following eigenvalue problems.

$$\left[s^2\mathbf{M}+s\mathbf{C}+\mathbf{K}\right]\mathbf{u} \;=\; \mathbf{0} \tag{7}$$

$$\left[2s\mathbf{M}+\mathbf{C}\right]\mathbf{u} \;=\; \mathbf{0} \tag{8}$$

The vector $\mathbf{Cu}$ is present in both equations, something that allows its elimination. This leads to a eigenvalue problem, still in terms of s but now without the viscous damping matrix

$$\left[-s^2\mathbf{M}+\mathbf{K}\right]\mathbf{u}=\mathbf{0} \tag{9}$$

Comparing this expression with the eigenvalue problem of an undamped system, it follows that the real and non-negative solutions of s which veryfies Eq. (9) are $s=-\omega_j$ for $1\leq j\leq n$. Plugging these solutions into Eq. (7), it yields the closed-form solutions of critical surfaces given by expression Eq. (6). As Papargyri-Beskou and Beskos [17] pointed out in their work "*thus the present method of determination of critical damping surfaces, even though approximate in the sense that there is no guarantee that $s_{cr}=-\omega_j$ corresponds to a minimum of damping, is much simpler computationally in comparison with the exact met hod of Boley and Beskos [5]*". In this section, a proof of the conditions to determine approximate critical surfase for nonvisoulsy damped systems will be addresed.

In order to establish the framework of the research, the general form of the damping model assumed in this paper will be described. The so-called exponential damping model is based on the assumptions that the effect of the dissipative forces depend on the time history of velocity response affected by a weight function (or also called hereditary) which exponentially backwards in time. From a physical point of view, exponentially damped structures present constitutive relationships based on the Zener 3-parameter viscoelastic model, or also called Standard Linear Solid [18](SLS model). The internal structure of these restraints is formed by linear springs and viscous dampers mathematically equivalent, in the Laplace domain, to rational relationships between stresses and strains [19]. This fact in turn leads to the aforementioned time-dependency between viscoelastic forces and the response via exponential kernels [20]

The general form of the hereditary damping function for a multiple dof system can be written, both in time and frequency domain, as

$$\boldsymbol{\mathcal{G}}(t)=\sum_{k=1}^{r}\mathbf{C}_k\,\mu_k\,e^{-\mu_k t} \quad , \quad \mathbf{G}(s)=\mathcal{L}\{\boldsymbol{\mathcal{G}}(t)\}=\sum_{k=1}^{r}\frac{\mu_k}{s+\mu_k}\mathbf{C}_k \tag{10}$$

where $\mu_k > 0$, $1 \leq k \leq r$ represent the relaxation or nonviscous parameters and $\mathbf{C}_k \in \mathbb{R}^{n\times n}$ are the symmetric damping matrices of the limit viscous model, obtained if the relaxation parameters tend to infinite, that is

$$\sum_{k=1}^{r} \mathbf{C}_k = \lim_{\mu_1 \ldots \mu_r \to \infty} \mathbf{G}(s) \tag{11}$$

The coefficients μ_k control the time– and frequency–dependence of the damping model while the spatial location and the level of damping are modeled via the matrices $\mathbf{C}_k$. It can easily be demonstrated that the damping function in the time domain and the limit damping coefficient are related by

$$\sum_{k=1}^{r} \mathbf{C}_k = \int_0^\infty \boldsymbol{\mathcal{G}}(t)\, dt \tag{12}$$

To the knowledge of the author, this paper presents the first approach to determine critical curves for multiple degree of freedom nonviscous systems. In this first attempt, the research will be focused on exponentially damped model whose time decay is controlled under just one nonviscous parameter, say $\mu_1 = \cdots = \mu_r \equiv \mu$. The numerical solution for the general case, with r distinct kernels, demands other different techniques which are currently under investigation. Thus, under these assumptions all viscous coefficients can be grouped in one viscous matrix $\mathbf{C}$ and the hereditary function under consideration can be written as

$$\boldsymbol{\mathcal{G}}(t) = \mathbf{C}\,\mu\, e^{-\mu t}\ , \quad \mathbf{G}(s) = \mathcal{L}\{\boldsymbol{\mathcal{G}}(t)\} = \frac{\mu}{s+\mu}\mathbf{C} \tag{13}$$

where $\mathcal{L}\{\bullet\}$ represents the Laplace trasnform, $\mu > 0$ the relaxation nonviscous parameter and $\mathbf{C} \in \mathbb{R}^{n\times n}$ is the (symmetric) matrix of the limit viscous damping model, defined as

$$\mathbf{C} = \lim_{\mu \to \infty} \mathbf{G}(s) \tag{14}$$

It will be assumed henceforth that $\mathbf{G}(s)$ depends not only on the eigenparameter s but also on a set of parameters that control dissipative behavior. Thus, the symmetric damping model presented in (13) depends at most on $N_{\max} = 1 + n(n+1)/2$ independent parameters. Indeed, $n(n+1)/2$ possible independent entrees within $\mathbf{C}$ plus the non–viscous parameter μ. Thus, the complete set of parameters can be listed as

$$\mu\ ,\ C_{11}\ ,\ C_{12}\ ,\ \ldots\ ,\ C_{n,n-1}\ ,\ C_{nn} \tag{15}$$

where $C_{ij} = C_{ji}$ is the ij-entree of $\mathbf{C}$, assumed symetric. Real applications depend in general on far fewer parameters, say $N << N_{\max}$. Simply to present a clearer exposition, the array $\boldsymbol{\theta} = \{\theta_1, \ldots, \theta_N\}$ denotes the set of independent damping parameters. Consequently, both the viscoelastic damping matrix and the dynamical stiffness matrix can be written as $\mathbf{G}(s, \boldsymbol{\theta})$ and $\mathbf{D}(s, \boldsymbol{\theta})$, respectively.

Let us consider now the following system of $n+1$ equations expressed in terms of the unknowns given by the $(n+1)$-tuple $(s, u_1, \ldots, u_n)$

$$\begin{aligned} F_j(s, u_1, \ldots, u_n, \boldsymbol{\theta}) &= \sum_{k=1}^{n} D_{jk}(s, \boldsymbol{\theta})\, u_k = 0\ , \quad 1 \leq j \leq n \\ F_{n+1}(s, u_1, \ldots, u_n, \boldsymbol{\theta}) &= f(u_1, \ldots, u_n) = 0 \end{aligned} \tag{16}$$

where $D_{jk}(s, \boldsymbol{\theta})$ is the entry (j,k) of the dynamical stiffness matrix $\mathbf{D}(s, \boldsymbol{\theta})$ and $f(u_1, \ldots, u_n)$ is a real valued function of the n components $u_1, \ldots, u_n$ which allows us to fix the eigenvector. Thus, suitable functions can be, for instance: $f(\mathbf{u}) = \sum_{k=1}^{n} u_k^2 - 1$ (unit vector), $f(\mathbf{u}) = \sum_{k=1}^{n}\sum_{j=1}^{n} u_j\, M_{jk}\, u_k - 1$ (mass normalized vector) or $f(\mathbf{u}) = u_j - 1$ (jth unit component). Eqs. (16) can be interpreted as a system of $n+1$ equations with $n+1$ unknowns depending on N parameters within $\boldsymbol{\theta}$. If the assigned values to $\boldsymbol{\theta}$ induce light damping in the system, then there exist n conjugate-complex eigensolutions of the form $(s_j, \mathbf{u}_j)$, $(s_j^*, \mathbf{u}_j^*)$, $1 \leq j \leq n$

and p real nonviscous eigenmodes $(s_j, \mathbf{u}_j)$, $2n+1 \leq j \leq 2n+p$, where $p = \text{rank}(\mathbf{C})$. As the parameters $\boldsymbol{\theta}$ increase the level of damping, some conjugate-complex pair will get closer to the negative real axis. The merging of a conjugate-complex pair into a one negative eigenvalue on the real axis is associated to a combination of the damping parameters $\boldsymbol{\theta}$, which lies exactly on a critical surface. Precisely at this point, the resulting negative eigenvalue is critical and double because it is root simultaneously of both Eqs. (5). If the level of damping continues to increase, then the $\boldsymbol{\theta}$ array will enters completely in the overdamped region and the double root will be divided into two overcritical eigenvalues.

Let us consider a particular combination of damping parameters $\boldsymbol{\theta} = \boldsymbol{\theta}_0$ lying inside the overdamped region. It is clear then that there exist at least two overdamped modes. Let us denote respectively by $s_0 \in \mathbb{R}^-$ and by $\mathbf{u}_0 \in \mathbb{R}^n$ to the eigenvalue and eigenvector of one of such modes. The $(n+1)-$tuple $(s_0, \mathbf{u}_0) \in \mathbb{R}^{n+1}$ can be read as a particular solution of Eq. (16). Small variations of $\boldsymbol{\theta}$ around $\boldsymbol{\theta}_0$ leads to a functional dependence of s and $\mathbf{u}$ with to $\boldsymbol{\theta}$. Mathematically, it is said then that there exist two functions

$$s = s(\boldsymbol{\theta}) : \mathbb{R}^N \to \mathbb{R} \ , \quad \mathbf{u} = \mathbf{u}(\boldsymbol{\theta}) : \mathbb{R}^N \to \mathbb{R}^n \tag{17}$$

which are implicitly defined by equations (16) around the point $(s_0, \mathbf{u}_0)$, and verifying $s_0 = s(\boldsymbol{\theta}_0)$ and $\mathbf{u}_0 = \mathbf{u}(\boldsymbol{\theta}_0)$. Additionally, it will be assumed as hypothesis that

$$\nabla f(\mathbf{u}_0) = \left\{ \frac{\partial f}{\partial u_1}, \ldots, \frac{\partial f}{\partial u_n} \right\}^T_{\mathbf{u}=\mathbf{u}_0} \neq \mathbf{0} \tag{18}$$

Sufficient conditions to guarantee the existence of the functions of Eqs (17) are provided by the implicit function theorem. Before addressing the application of this theorem for our particular case, equations and variables will be presented in a more compact form, for the sake of clarity. Thus, those variables candidates to be defined as functions can be arranged in the array $\mathbf{y} = (s, \mathbf{u}) \in \mathbb{R}^{n+1}$, thus the $n+1$ equations (16) can be expressed simply as $\mathbf{F}(\mathbf{y}, \boldsymbol{\theta}) = \mathbf{0}$, where $\mathbf{F}(\mathbf{y}, \boldsymbol{\theta}) : \mathbb{R}^{n+1+N} \to \mathbb{R}^{n+1}$ is

$$\mathbf{F}(\mathbf{y}, \boldsymbol{\theta}) = \{F_1(\mathbf{y}, \boldsymbol{\theta}), \ldots, F_n(\mathbf{y}, \boldsymbol{\theta}), F_{n+1}(\mathbf{y}, \boldsymbol{\theta})\}^T \tag{19}$$

Assuming that $\mathbf{F}(\mathbf{y}, \boldsymbol{\theta})$ is a continuously differentiable function in a neighboorhood of $(\mathbf{y}_0, \boldsymbol{\theta}_0)$, where $\mathbf{y_0} = \{s_0, \mathbf{u}_0\}^T$ and $\mathbf{F}(\mathbf{y}_0, \boldsymbol{\theta}_0) = \mathbf{0}$, then if the Jacobian matrix $\boldsymbol{\mathcal{J}}_{\mathbf{F},\mathbf{y}}(\mathbf{y}_0, \boldsymbol{\theta}_0)$ is invertible, it can be ensured that there exists an open set $U \subset \mathbb{R}^N$ around $\boldsymbol{\theta}_0$ and a unique continuously differentiable function $\mathbf{y} = \mathbf{g}(\boldsymbol{\theta}) : U \to \mathbb{R}^{n+1}$, such that $\mathbf{g}(\boldsymbol{\theta}_0) = \mathbf{y}_0$ and $\mathbf{F}(\mathbf{g}(\boldsymbol{\theta}), \boldsymbol{\theta}) = \mathbf{0}$ for all $\boldsymbol{\theta} \in U$. If, otherwise, $\boldsymbol{\theta}_0$ lies on a critical surface, these functions will be not properly defined since small variations of the damping parameters will lead the system to indefinite state with two possible conjugate complex solutions. Surveying under what conditions the Jacobian matrix becomes non–invertible will provide additional information for overcritical damping. According to the definition of the Jacobian matrix, we have

$$\boldsymbol{\mathcal{J}}_{\mathbf{F},\mathbf{y}} = \left[\frac{\partial \mathbf{F}}{\partial \mathbf{y}}\right] = \left[\begin{array}{c|ccc} \frac{\partial F_1}{\partial s} & \frac{\partial F_1}{\partial u_1} & \cdots & \frac{\partial F_1}{\partial u_n} \\ \frac{\partial F_2}{\partial s} & \frac{\partial F_2}{\partial u_1} & \cdots & \frac{\partial F_2}{\partial u_n} \\ \vdots & \vdots & \ddots & \vdots \\ \frac{\partial F_n}{\partial s} & \frac{\partial F_n}{\partial u_1} & \cdots & \frac{\partial F_n}{\partial u_n} \\ \hline \frac{\partial F_{n+1}}{\partial s} & \frac{\partial F_{n+1}}{\partial u_1} & \cdots & \frac{\partial F_{n+1}}{\partial u_n} \end{array}\right] = \left[\begin{array}{c|c} \dfrac{\partial \mathbf{D}}{\partial s}\mathbf{u} & \mathbf{D} \\ \hline 0 & \boldsymbol{\nabla}^T f \end{array}\right] \in \mathbb{R}^{(n+1)\times(n+1)} \tag{20}$$

This result shows that the Jacobian matrix is formed by four matrix blocks. Assuming $(s, \mathbf{u}) \in \mathbb{R}^{n+1}$, then $\frac{\partial \mathbf{D}}{\partial s}\mathbf{u} \in \mathbb{R}^n$ is a column vector, $\mathbf{D}(s, \boldsymbol{\theta}) \in \mathbb{R}^{n\times n}$ is the dynamic stiffness matrix and $\boldsymbol{\nabla} f \in \mathbb{R}^n$ represents the gradient of $f(u_1, \ldots, u_n)$ in column. Since s_0 is an eigenvalue, it is clear that $\text{rank}\,[\mathbf{D}(s_0, \boldsymbol{\theta}_0)] = n-1$. If we assume that $\boldsymbol{\nabla} f$ is linearly independent of the columns of $\mathbf{D}(s_0, \boldsymbol{\theta}_0)$, then $\text{rank}\,[\mathbf{D}\ \nabla f] = n$. Therefore,

if $\frac{\partial \mathbf{D}}{\partial s}\mathbf{u} = 0$ at $(s_0, \mathbf{u}_0, \boldsymbol{\theta}_0)$, then the functions $s(\boldsymbol{\theta})$ and $\mathbf{u}(\boldsymbol{\theta})$ are not univocally defined and this point $\boldsymbol{\theta}_0$ is candidate to lie on a critical surface, which is precisely our goal. Therefore, critical eigenvalues will be solutions that will simultaneously verify the following two eigenvalue problems

$$\mathbf{D}(s,\boldsymbol{\theta})\,\mathbf{u} = \left[s^2\mathbf{M} + s\mathbf{G}(s,\boldsymbol{\theta}) + \mathbf{K}\right]\mathbf{u} = \mathbf{0} \tag{21}$$

$$\frac{\partial \mathbf{D}}{\partial s}\,\mathbf{u} = \left[2s\mathbf{M} + \mathbf{G}(s,\boldsymbol{\theta}) + s\mathbf{G}'(s,\boldsymbol{\theta})\right]\mathbf{u} = \mathbf{0} \tag{22}$$

where $(\bullet)' = \partial(\bullet)/\partial s$. The derived condition (22) is not equivalent to $\frac{\partial}{\partial s}\det\left[\mathbf{D}(s)\right] = 0$, therefore the so found real eigenvalues will not correspond to a minimum of damping. Consequently, according to the reference [17], the obtained critical surface will be an approximation of the exact one. Furthermore, if the approximate eigenvalue is not exactly critical, obviously it will lie inside the exact overdamped region, thus the proposed method lead to conservative results. This fact will be visualized in the numerical examples.

Now, following the same procedure carried out by Papargyri-Beskou and Beskos [17] for viscous systems, it seems reasonable to eliminate damping matrices in order to find eigenvalues just as solutions of mass and stiffness matrices. However, for nonviscous systems this is not straightforward since not only $\mathbf{G}(s)$ but also $\mathbf{G}'(s)$ is involved in Eq. (22). In this paper, satisfactory results have been accomplished considering exponentially damped systems over one hereditary kernel, which general form yields

$$\mathbf{G}(s) = \frac{\mu}{s+\mu}\mathbf{C} \equiv g(s)\,\mathbf{C} \tag{23}$$

where $g(s) = \mu/(s+\mu)$ denotes the frequency–dependent part of the damping model and $\mathbf{C}$ is the limit viscous matrix. Assuming then the damping model of Eq. (23), Eqs. (21) and (22) yield

$$\left[s^2\mathbf{M} + s\,g(s)\,\mathbf{C} + \mathbf{K}\right]\mathbf{u} = \mathbf{0} \tag{24}$$

$$\left[2s\mathbf{M} + g(s)\,\mathbf{C} + s\,g'(s)\,\mathbf{C}\right]\mathbf{u} = \mathbf{0} \tag{25}$$

where, for the sake of simplicity, explicit dependence on the parameters $\boldsymbol{\theta}$ has been omitted because it results irrelevant for the forthcoming developments. Dividing Eqs. (24) and (25) by $s\,g(s)$ and $g(s)+s\,g'(s)$, respectively, and subtracting both results, yields

$$\left[\left(\frac{s^2}{sg(s)} - \frac{2s}{g(s)+sg'(s)}\right)\mathbf{M} + \frac{1}{s\,g(s)}\,\mathbf{K}\right]\mathbf{u} = \mathbf{0} \tag{26}$$

After some straight operations this equation can be rearranged in a more compact form

$$\left[-s^2\,\frac{g(s) - s\,g'(s)}{g(s) + s\,g'(s)}\,\mathbf{M} + \mathbf{K}\right]\mathbf{u} = \mathbf{0} \tag{27}$$

Comparing now this eigenvalue problem in s with the undamped problem

$$\left[-\omega_j^2\,\mathbf{M} + \mathbf{K}\right]\boldsymbol{\phi}_j = \mathbf{0} \tag{28}$$

it can be concluded that, if s_{cr} is a negative and real solution of the equation

$$s^2\,\frac{g(s) - s\,g'(s)}{g(s) + s\,g'(s)} = \omega_j^2 \tag{29}$$

then the following expression represents an approximate critical surface

$$\det\left[s_{cr}^2\mathbf{M} + s_{cr}\,\mathbf{G}(s_{cr}) + \mathbf{K}\right] = 0 \tag{30}$$

In order to define properly a critical surface, note that the value s_{cr} must be plugged into the above equation as function of the damping parameters, namely, s in Eq. (29) must be analytically solved as a closed form

of the parameter μ. Henceforth, we will refer to Eq. (29) as the *jth critical modal equation* or just as *critical equation* when there is no room for confusion. Eq. (29) can be interpreted as a generalization of that for viscous damping. Indeed, for viscous damping yields $g'(s) \equiv 0$, leading to $s^2 = \omega_j^2$, equation already obtained by Papargyri-Beskou and Beskos [17]. Critical solutions for this equation are, as know, $s = -\omega_j$, leading to Eqs. (6) as the critical surfaces for viscous systems. For nonviscous damping, this simple equation is somehow perturbed adopting the form of Eq. (29). For $g(s) = \mu/(s+\mu)$ and after some straight operations, the critical equation (29) turns in to the third order polynomial

$$\left(\frac{s}{\omega_j}\right)^2 \left(1 + \frac{2s}{\mu}\right) = 1 \quad , \quad 1 \leq j \leq n \tag{31}$$

It is known that the three roots of this equation are analytically available as closed forms of the polynomial coefficients. If, among them, those negative can be distinguished (remind that we are trying to find functions, not numbers), then they will be approximations of critical eigenvalues and consequently can be introduced into Eq. (30) to determine approaches of critical surfaces. As will be seen in the next point, the jth modal critical equation of a multiple dof system coincides with that of a single dof system with natural frequency ω_j. Hence, the derivation of the critical eigenvalues is closely related to the analysis of the already known critical curves of a single dof viscoelastic oscillator [14].

3. Single degree-of-freedom systems

The critical damping region of a single dof exponentially nonviscouly oscillator play an important role in the development of a more general model for multi degree freedom systems. Consequently, the main results will be revisited at this point. Let $u(t)$ denote the single degree of freedom (schematically represented by the displacement of certain mass m attached to ground by the viscoelastic constraint), then the free equation of motion can be deduced from the dynamic equilibrium

$$m\ddot{u} + \int_{-\infty}^{t} \mathcal{G}(t-\tau)\dot{u}(\tau)\mathrm{d}\tau + ku(t) = 0 \tag{32}$$

where k is the constant of the linear-elastic spring and $\mathcal{G}(t)$ is the hereditary kernel expressed both in time and frequency domain as

$$\mathcal{G}(t) = c\,\mu\, e^{-\mu t} \ , \quad G(s) = \frac{\mu\, c}{s+\mu} \tag{33}$$

where μ and c are the relaxation parameter and the viscous coefficient, respectively. The characteristic equation yields

$$D(s) = ms^2 + s\,G(s) + k = ms^2 + s\frac{\mu\, c}{s+\mu} + k = 0 \tag{34}$$

The additional condition of critical damping yields [6]

$$\frac{\partial D}{\partial s} = 2\,m\,s + G(s) + s\,G'(s) = 2\,m\,s + \left(\frac{\mu}{s+\mu} - \frac{\mu}{(s+\mu)^2}\right) c = 0 \tag{35}$$

Eliminating parameter c form Eqs. (34) and (35) one finds

$$\left(\frac{s}{\omega_n}\right)^2 \left(1 + \frac{2s}{\mu}\right) = 1 \tag{36}$$

where $\omega_n = \sqrt{k/m}$. By comparison of the above expression with that of Eq. (31), it follows that the jth modal critical equation has exactly the same structure of that of a single dof system with natural frequency ω_j. The well known critical curves of the single dof system will help us to interpret the solutions for the jth critical equation of a multiple dof system. Thus, it is suitable to define several dimensionless variables

$$x = \frac{s}{\omega_n} \ , \quad \nu = \frac{\omega_n}{\mu} \ , \quad \zeta = \frac{c}{2m\omega_n} \tag{37}$$

Eq. (36) can then be written as

$$x^2\,(1+2\,\nu\,x)=1 \tag{38}$$

The three roots are available from the Cardano's formulas as functions of the nonviscous parameter ν. After the shift in the variable $x = X - 1/6\nu$, the third order polynomial can be expressed in the normal form

$$X^3 + a\,X + b = 0 \tag{39}$$

where

$$a = -\frac{1}{12\nu^2}\ , \quad b = \frac{1-54\nu^2}{108\nu^3} \tag{40}$$

The discriminant that controls the nature of the roots becomes

$$\Delta = b^2 + \frac{4}{27}a^3 = \frac{27\nu^2-1}{108\nu^4} \tag{41}$$

If $\Delta > 0$, then the polynomial has two conjugate-complex solutions and one real. If, otherwise, $\Delta \leq 0$, then the three roots are real. Within the latter case, the three real eigenvalues are distinct if stricly $\Delta < 0$. Imposing this condition, critical solutions always lie in the interval $0 \leq \nu \leq 1/3\sqrt{3}$, interval that coincides with that one derived by Adhikari [14]. Assuming then that $0 \leq \nu \leq 1/3\sqrt{3}$, the three roots can be expressed as [21]

$$\begin{aligned}
x_1(\nu) &= 2\sqrt{\frac{-a}{3}}\,\cos\left(\frac{\theta(\nu)}{3}\right) - \frac{1}{6\nu} = \frac{1}{3\nu}\left[\cos\left(\frac{\theta(\nu)}{3}\right) - \frac{1}{2}\right] \\
x_2(\nu) &= 2\sqrt{\frac{-a}{3}}\,\cos\left(\frac{\theta(\nu)+2\pi}{3}\right) - \frac{1}{6\nu} = \frac{1}{3\nu}\left[\cos\left(\frac{\theta(\nu)+2\pi}{3}\right) - \frac{1}{2}\right] \\
x_3(\nu) &= 2\sqrt{\frac{-a}{3}}\,\cos\left(\frac{\theta(\nu)+4\pi}{3}\right) - \frac{1}{6\nu} = \frac{1}{3\nu}\left[\cos\left(\frac{\theta(\nu)+4\pi}{3}\right) - \frac{1}{2}\right]
\end{aligned} \tag{42}$$

where

$$\theta(\nu) = \arccos\left(-\frac{b}{2}\sqrt{-\frac{27}{a^3}}\right) = \arccos\left(54\nu^2-1\right) \in [0,\pi] \tag{43}$$

The graph of the three roots with ν has been plotted in Fig. 1 (top-left). It can be observed that the inequalities

$$x_2(\nu) < x_3(\nu) < 0 < x_1(\nu) \tag{44}$$

hold in the range $0 \leq \nu < 1/3\sqrt{3}$. Therefore, $x_1(\nu)$ can be discarded since is positive. Negative roots are distributed along curves $x_2(\nu)$ and $x_3(\nu)$ which are actually two branches of the same continuous curve, as noticed in Fig. 1(top-left), with the common point at $\nu = 1/3\sqrt{3}$.

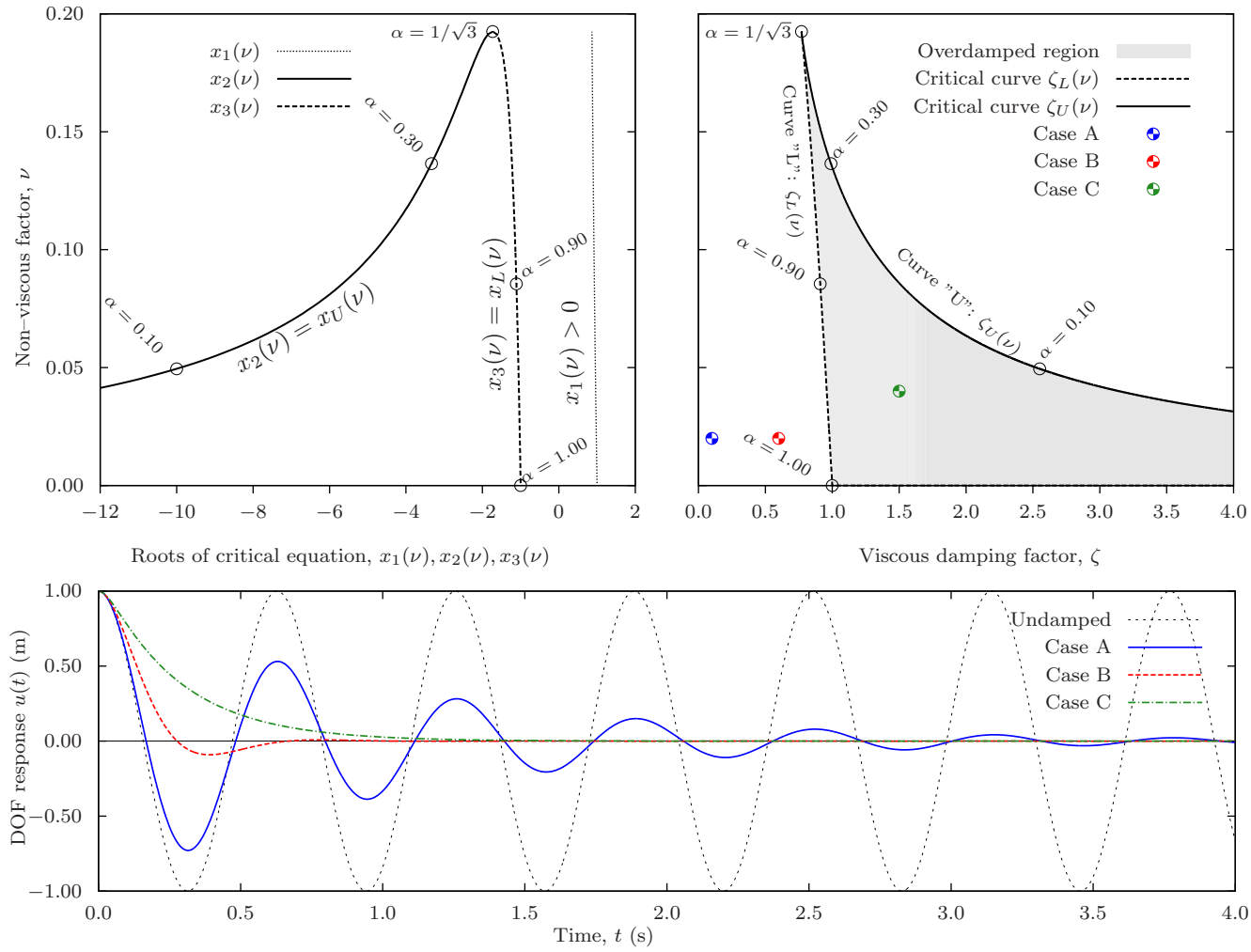

Figure 1: Top-left: roots of the critical equation in dimensionless form $x = s/\omega_n$ for the single degree-of-freedom oscillator. Top-right: Critical damping region in the (ζ, ν) domain. Parameter α is defined as $\alpha = -\omega_n/x$. Bottom: Time-domain response $u(t)$ for a single dof system with $\omega_r = 10$ rad/s under the three damping cases shown in top-right plot (A, B and C) together with the undamped case; initial values $u(0) = 1,\ \dot{u}(0) = 0$

Plugging $s = x_2(\nu)\omega_n$ and $s = x_3(\nu)\omega_n$ into Eq. (34) (or into Eq. (35), with same result), critical viscous damping coefficient $c_{cr}(\nu)$ can be solved in terms of ν. Traditionally, this result is preferably given in terms of the dimensionless damping ratio $\zeta = c/2m\omega_n$. Thus, after some simplifications the two critical damping ratios can be obtained as

$$\zeta_L(\nu) = -\frac{1+\nu\, x_3(\nu)}{2x_3(\nu)}\left[1+x_3^2(\nu)\right] \quad , \qquad \zeta_U(\nu) = -\frac{1+\nu\, x_2(\nu)}{2x_2(\nu)}\left[1+x_2^2(\nu)\right] \tag{45}$$

where the same notation as Ref. [14] has been used to denote the lower, ζ_L, and the upper ,ζ_U, critical damping ratios. Hence, the overdamped region can mathematically be defined as

$$\left\{(\zeta,\nu) \in \mathbb{R}^2 : \zeta_L(\nu) \le \zeta \le \zeta_U(\nu)\ ,\ 0 \le \nu \le 1/3\sqrt{3}\right\} \tag{46}$$

and has been plotted in Fig. 1(top-right). By extension, the same notation for the critical eigenvalues will

be adopted. Thus, the functions

$$x_L(\nu) = x_3(\nu) \ , \quad x_U(\nu) = x_2(\nu) \tag{47}$$

denote the critical eigenvalues with which the damping ratios $\zeta_L(\nu)$ and $\zeta_U(\nu)$ are determined in Eq. (45), respectively.

As proved above, and observed in Fig. 1(top-right), the overdamped region is enclosed by the two curves $\zeta_L(\nu)$ and $\zeta_U(\nu)$, both evaluated from Eqs. (45) as function of the nonviscous factor ν. This latter should be interpreted as an independent variable within the interval $0 \leq \nu \leq 1/3\sqrt{3}$. It is said then that the entire critical curve is presented as the union of two graphs. It turns out that it is possible to define a real parameter, say $\alpha \in \mathbb{R}$ within certain interval $I \subset \mathbb{R}$ and to find two expressions $\zeta(\alpha)$ and $\nu(\alpha)$ such that the set of points $\{(\zeta(\alpha), \nu(\alpha)), \alpha \in I\}$ is precisely the critical curve. The main idea is to read $x \in \mathbb{R}^-$ in Eq. (38) as a parameter, instead as an unknown. Thus, solving for ν as function of x in Eq. (38), yields

$$\nu = \frac{1 - x^2}{2x^3} \ , \quad -\infty < x \leq -1 \tag{48}$$

As x varies in the interval $-\infty < x \leq -1$, the nonviscous factor lies within the interval $\nu \in \left[0, 1/3\sqrt{3}\right]$. As seen before, for each ν two values of x can be found and, consequently, two values of ζ arise. But inverting the order of dependency, for each $x \in (-\infty, -1]$ one and only one ν is found and, from Eq. (34), one and only one damping ratio is obtained. Indeed, plugging Eq. (48) into Eq. (34) and solving for $\zeta = c/2m\omega_n$, yields

$$\zeta = -\frac{\left(x^2 + 1\right)^2}{4x^3} \ , \quad -\infty < x \leq -1 \tag{49}$$

If the parameter α is chosen as $\alpha = -1/x$, then Eqs. (48) and (49) yield

$$\zeta_c(\alpha) = \frac{\left(\alpha^2 + 1\right)^2}{4\alpha} \ , \quad \nu_c(\alpha) = \frac{1}{2}\alpha\left(1 - \alpha^2\right) \ , \quad 0 < \alpha \leq 1 \tag{50}$$

Both expressions define parametrically the critical curve in the interval $\alpha \in (0, 1]$. Moreover, the set of points $(\nu, \zeta_L(\nu))$ and $(\nu, \zeta_U(\nu))$ are associated to two different subintervals in the range of α, say

$$\begin{aligned} \left\{(\nu, \zeta_U(\nu)) : 0 \leq \nu \leq 1/3\sqrt{3}\right\} &= \left\{(\nu_c(\alpha), \zeta_c(\alpha)) : 0 < \alpha \leq 1/\sqrt{3}\right\} \\ \left\{(\nu, \zeta_L(\nu)) : 0 \leq \nu \leq 1/3\sqrt{3}\right\} &= \left\{(\nu_c(\alpha), \zeta_c(\alpha)) : 1/\sqrt{3} \leq \alpha \leq 1\right\} \end{aligned} \tag{51}$$

In the Fig. 1(top-left and top-right), the parameter α has been evaluated at $\alpha = \left\{0.10, 0.30, 1/\sqrt{3}, 0.90, 1.00\right\}$ and the corresponding points have been plotted along the curves. That point associated to $\alpha \to 0$ corresponds to the infinite point at the end of the asymptotic branch $(\zeta, \nu) = (+\infty, 0)$. On the oposite edge, the point $\alpha = 1$ is located on the ζ-axis, form $\nu = 0$ and it makes reference to the limit viscous state. As will be justified later, it turns out that this form of setting the critical curve using this new parameter α results more suitable for achieving the main objective: to determine critical curves in multiple degree-of-freedom systems, something that will be carried out in the next point. As known, the choice of the damping parameters strongly affects to the nature of time response. By definition, any pair (ζ, ν) lying within the overdamped region led the system to a pure exponential decay in unforced problems. In order to visualize this behavior, several time-domain simulations have been plotted in the Fig.1 (bottom). The integration has been carried out using the state-space method together with the initial conditions $u(0) = 1, \ \dot{u}(0) = 0$ and considering no external force applied. Four different cases have been simulated: case with no damping, case A (light damping, $\zeta = 0.1, \ \nu = 0.02$) and case B (high damping, $\zeta = 0.6, \ \nu = 0.02$) and case B (overcritical damping, $\zeta = 1.5, \ \nu = 0.04$). Case A and the undamped one present approximately the same frequency since the former can be considered as lightly damped. Case B presents oscillatory motion since it lies outside the critical region but hardly one cicle is percibed due to the high exponential decay. Finally, case C represents an overdamped behavior and, as expected, its time-domain response does not present oscillations, decaying

(exponentially) almost completely within the first second from the initial value $u(0) = 1$. As will be seen in the next point, in systems with multiple degrees of freedom, the phenomenon of overcritical damping may affect differently each one of the modes.

4. Multiple degree–of–freedom systems

In this section, the application of the proposed method tononviscously damped systems with multiple degrees of freedom will be addressed. As established in the above theoretical derivations, the viscoelastic damping matrix is assumed to obey a Biot's exponential model with one hereditary kernel, say

$$\boldsymbol{\mathcal{G}}(t) = \mu\, e^{-\mu t}\, \mathbf{C} \quad , \qquad \mathbf{G}(s) = \frac{\mu}{s+\mu}\, \mathbf{C} \tag{52}$$

where $\mu \in \mathbb{R}$ is the relaxation parameter and $\mathbf{C}$ is the viscous matrix. According to Eq. (31), if ω_j denotes the jth natural frequency of the undamped system, the set of approximate critical eigenvalues associated to the jth mode verifies the critical equation

$$\left(\frac{s}{\omega_j}\right)^2 \left(1 + \frac{2s}{\mu}\right) = 1 \quad , \quad 1 \leq j \leq n \tag{53}$$

Additionally, these eigenvalues lie in the interval $-\infty < s \leq -\omega_j$ as proved above for single dof systems. Thus, approximate critical surfaces are expressions that depend only on the damping parameters and are determined as a result of eliminating s from Eq. (53) and

$$\det\left[s^2\mathbf{M} + s\,\mathbf{G}(s) + \mathbf{K}\right] = 0 \tag{54}$$

Expressions of s as function of μ are available from Secc. 3. The approximate critical eigenvalues are solutions of the modal critical equation (53). While in Eqs.(47) the input-argument in functions $x_L(\nu)$ and $x_U(\nu)$ was $\nu = \omega_n/\mu$, at the current point this role is played by the ratio ω_j/μ and therefore these functions must be calculated for each mode. They can be lined up along two curves denoted as type "L" and "U" followed by the mode index j, i.e. Lj and Uj.

$$\begin{aligned} \text{Critical eigenvalues of curve } Lj \quad &: \quad s_{Lj}(\mu) = x_L(\omega_j/\mu)\,\omega_j \\ \text{Critical eigenvalues of curve } Uj \quad &: \quad s_{Uj}(\mu) = x_U(\omega_j/\mu)\,\omega_j \end{aligned} \tag{55}$$

where the functions $x_L(\nu)$ and $x_U(\nu)$ have been defined in Eqs. (47) and (42) in the range $0 \leq \nu \leq 1/3\sqrt{3}$. Therefore, the operational range of the parameter μ varies with the considered mode, being in general

$$\frac{\omega_j}{\mu} \leq \frac{1}{3\sqrt{3}} \tag{56}$$

Now, once the critical eigenvalues are determined, the associated critical curves can be built for each mode as

$$\begin{aligned} \text{Critical curves } Lj \quad &: \quad \det\left[s_{Lj}^2(\mu)\,\mathbf{M} + \frac{s_{Lj}(\mu)\,\mu}{s_{Lj}(\mu)+\mu}\,\mathbf{C} + \mathbf{K}\right] \equiv \mathcal{L}_j(\mu, \mathbf{C}) = 0 \;, \quad 1 \leq j \leq n \\ \text{Critical curves } Uj \quad &: \quad \det\left[s_{Uj}^2(\mu)\,\mathbf{M} + \frac{s_{Uj}(\mu)\,\mu}{s_{Uj}(\mu)+\mu}\,\mathbf{C} + \mathbf{K}\right] \equiv \mathcal{U}_j(\mu, \mathbf{C}) = 0 \;, \quad 1 \leq j \leq n \end{aligned} \tag{57}$$

The two expressions $\mathcal{L}_j(\mu, \mathbf{C}) = 0$ and $\mathcal{U}_j(\mu, \mathbf{C}) = 0$ implicitly define one piecewise surface in the domain of the damping parameters. Moreover, both equations coincide for $\mu = 3\sqrt{3}\omega_j$. The region enclosed by these surfaces (curves if only two damping parameters are involved) are candidate to define the approximate overdamped region of the system. Since our method is not exact, the proposed critical curves do not correspond to a minimum damping. Therefore, the proposed critical eigenvalues lie actually inside the

exact critical region or, in other words, the approximate critical regions are conservative approaches of the exact ones. Those former are enveloped by the latter, something that can also be observed in purely viscous systems [7, 17].

The solutions of the critical equation, in terms of μ result in the piecewise functions defined by $s_{Lj}(\mu)$ and $s_{Uj}(\mu)$ presented above. It has been already discussed that, besides this procedure, the critical curve for single dof systems can be constructed using a parametric formulation, see Eqs. (50). Let us see now that, following this approach, to find the critical curves can be carried out much more efficiently for multiple dof systems using a local parameter. In this way, the computation of the determinants of Eqs. (57) is avoided, improving notably the computational cost specially for larger systems.

Let us consider the parameter $\alpha = -\omega_j/s$ in Eq. (53). As previously proved, the set of negative roots are within the interval $-\infty < s < -\omega_j$. Therefore, the parameter α is defined in the range $0 < \alpha \leq 1$. In terms of α, the nonviscous parameter yields

$$\frac{\omega_j}{\mu} = \frac{\alpha}{2}\left(1-\alpha^2\right) \tag{58}$$

This expression is an extension of that of Eq. (50) for the jth mode. Now, plugging Eq. (58) into Eq. (7) together with $s = -\omega_j/\alpha$, it yields

$$\left[\frac{\omega_j^2}{\alpha^2}\mathbf{M} - \frac{2\omega_j}{\alpha(1+\alpha^2)}\mathbf{C} + \mathbf{K}\right]\,\mathbf{u} = \mathbf{0} \tag{59}$$

After some straight operations, Eq. (59) can be written as

$$\left[\mathbf{A}_j(\alpha) - \mathbf{C}\right]\,\mathbf{u} = \mathbf{0} \tag{60}$$

where,

$$\mathbf{A}_j(\alpha) = \frac{1+\alpha^2}{2\omega_j\alpha}\left(\omega_j^2\mathbf{M} + \alpha^2\,\mathbf{K}\right)\ , \quad 0 < \alpha \leq 1 \tag{61}$$

If, for instance, we are interested in determining the critical region that relates the relaxation parameter μ and certain viscous coefficient c within $\mathbf{C}$, then Eq. (60) can be read as a linear eigenvalue problem in terms of c. Indeed,

$$\left[\mathbf{A}_j(\alpha) - c\,\mathbf{J}\right]\,\mathbf{u} = \mathbf{0} \tag{62}$$

where $\mathbf{J} = \mathbf{C}/c = [C_{ij}/c]$. If $p = \text{rank}(\mathbf{C})$, then for each value of $\alpha \in (0, 1]$ we obtain p finite nonzero eigenvalues and a infinite eigenvalue with multiplicity $n - p$. Thus, the spectral set can be expressed as

$$\underbrace{c_{j1}(\alpha)\ ,\ \cdots\ ,\ c_{jp}(\alpha)}_{p}\ ,\ \underbrace{\infty\ ,\ \cdots\ ,\ \infty}_{n-p} \tag{63}$$

Therefore, for each mode j, with $1 \leq j \leq n$, p curves in parametric form defined in the domain (μ, c) can be determined, say

$$\left\{(\mu_j(\alpha), c_{j1}(\alpha))\ ,\quad 0 < \alpha \leq 1\right\}\ ,\ \cdots\ ,\ \left\{(\mu_j(\alpha), c_{jp}(\alpha))\ ,\quad 0 < \alpha \leq 1\right\} \tag{64}$$

where, for all of them

$$\mu_j(\alpha) = \frac{2\omega_j}{\alpha\left(1-\alpha^2\right)}\ , \quad 1 \leq j \leq n \tag{65}$$

As will be shown in the numerical examples, overdamped regions are somehow enclosed by the so obtained critical curves. The proof of the critical damping conditions using the implicit function theorem (Section 2), the derivation of the critical modal equations (31) and the numerical method to determine approximate critical curves for multiple dof systems (Section 4) are considered the most important contributions of this paper. Now, in the next Sections, the theoretical derivations will be validated throughout two numerical examples where the procedure to determine the overdamped regions will be described in detail.

5. Numerical example 1: Discrete system

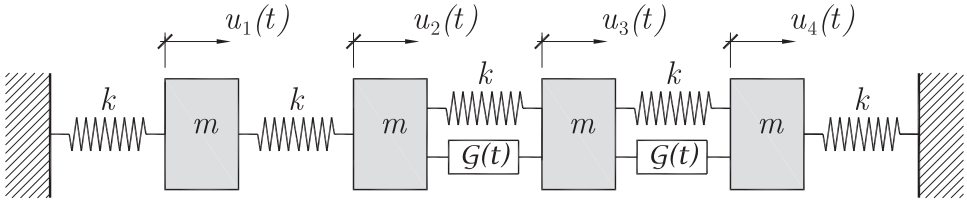

Figure 2: Example 1: The four degrees–of–freedom discrete system. $\mathcal{G}(t)$ represents the hereditary function of nonviscous dampers. Masses $m = 10$ kg, Rigidities $k = 10^3$ N/m.

In the first example, a discrete lumped-parameter system with four degrees of freedom will be considered. Fig. 2 represents the distribution of the four masses $m = 10$ kg, constrained with linear rigidities $k = 10^3$ N/m and two viscoelastic dampers modeled with a hereditary function $\mathcal{G}(t) = c\,\mu\,e^{-\mu t}$, where c denotes limit viscous damping coefficient and μ the nonviscous relaxation parameter. According to this configuration, the mass matrix of the system is $\mathbf{M} = m\mathbf{I}_4$ and the stiffness and damping matrix yield

$$\mathbf{K} = k\begin{bmatrix} 2 & -1 & 0 & 0 \\ -1 & 2 & -1 & 0 \\ 0 & -1 & 2 & -1 \\ 0 & 0 & -1 & 2 \end{bmatrix} = \qquad , \quad \boldsymbol{\mathcal{G}}(t) = \mu e^{-\mu t}\begin{bmatrix} 0 & 0 & 0 & 0 \\ 0 & c & -c & 0 \\ 0 & -c & 2c & -c \\ 0 & 0 & -c & c \end{bmatrix} \tag{66}$$

The main goal is to find the critical curves in terms of the damping parameters (c, μ). As carried out for single dof systems, these parameters will be expressed in nondimensional form as

$$\zeta = \frac{c}{2m\omega_r} \ , \quad \nu = \frac{\omega_r}{\mu} \tag{67}$$

and defined respect to a reference frequency, in this case $\omega_r = \sqrt{k/m} = 10$ rad/s. Since the critical curves are constructed using the undamped frequencies, the linear eigenvalue problem $\left(-\omega^2\mathbf{M} + \mathbf{K}\right)\mathbf{u} = \mathbf{0}$ needs to be solved, whose results are shown in Table 1 respect to the reference frequency. The next step

k (N/m)	m (kg)	ω_1/ω_r	ω_2/ω_r	ω_3/ω_r	ω_4/ω_r
10^3	10.00	0.618034	1.17557	1.61803	1.90211

Table 1: Example 1: Numerical example natural frequencies

is to obtain the solutions of each modal critical equation. As the theoretical developments have shown, dimensionless solutions of the jth critical equations s/ω_j, see Eqs. (55), depend uniquely on the modal nonviscous parameter ω_j/μ which in turn can be expressed as

$$\frac{\omega_j}{\mu} = \frac{\omega_j}{\omega_r}\frac{\omega_r}{\mu} = \frac{\omega_j}{\omega_r}\,\nu$$

Thus, the critical eigenvalues associated to the jth mode are

$$s_{Lj}(\nu) = \frac{\omega_r}{3\nu}\left[\cos\left(\frac{\theta(\omega_j\nu/\omega_r) + 2\pi}{3}\right) - \frac{1}{2}\right] \ , \quad 1 \le j \le 4 \tag{68}$$

$$s_{Uj}(\nu) = \frac{\omega_r}{3\nu}\left[\cos\left(\frac{\theta(\omega_j\nu/\omega_r) + 4\pi}{3}\right) - \frac{1}{2}\right] \ , \quad 1 \le j \le 4 \tag{69}$$

where the function $\theta(\bullet)$ has already been defined in Eq. (43). A family of candidate critical curves can be found plugging both Eqs. (68) and (69) into the expression of the determinant of the system, leading to Eqs. (57). In general, this expression adopts the form of a polynomial in the parameter ζ. The maximum order of this polynomial directly depends on the rank of the damping matrix. Since $\operatorname{rank}(\mathbf{C}) = 2$ then the equation $\det[\mathbf{D}(s)] = 0$ can be expressed as

$$\det[\mathbf{D}(s)] = p_0(s,\nu) + p_1(s,\nu)\,\zeta + p_2(s,\nu)\,\zeta^2 = 0 \tag{70}$$

where $p_0,\ p_1,\ p_2$ are in turn polynomials in s and ν. Substituting the value of s in the above equation by $s_{Lj}(\nu)$, from Eq. (68), ~~into Eq. (70),~~ two possible solutions of ζ can be found for each ν (in general, p values would be obtained, with $p = \operatorname{rank}\mathbf{C}$). These solutions are in fact two curves, $\zeta_{Lj}^{(1)}(\nu)$ and $\zeta_{Lj}^{(2)}(\nu)$, which represent the lower bounds of the critical regions associated to the jth mode. Similarly, $s_{Uj}(\nu)$ results in other two solutions of Eq. (70), say $\zeta_{Uj}^{(1)}(\nu), \zeta_{Uj}^{(2)}(\nu)$, and they form the upper bounds of the critical regions. Thus, the critical region, associated to the mode j can be defined as

$$\bigcup_{i=1}^{p} \left\{ (\zeta,\nu) \in \mathbb{R}^2 : \zeta_{Lj}^{(i)}(\nu) \le \zeta \le \zeta_{Uj}^{(i)}(\nu)\ ,\ 0 \le \nu \le \nu_{\max,j} = \frac{\omega_r}{3\sqrt{3}\omega_j} \right\} \tag{71}$$

For this example, the number of degrees of freedom is $n = 4$ and the rank of the damping matrix is $p = 2$, therefore $n \times p = 8$ critical curves can be drawn. In the Fig. 3 these curves have been plotted together with the exact critical curves. These latter have been determined using the method developed in the Ref. [6]. For each mode, the two functions $\zeta_{Lj}^{(i)}(\nu)$ and $\zeta_{Uj}^{(i)}(\nu)$ present a common point at $\nu = 1/3\sqrt{3}\omega_j$. Thus, if they are considered as two branches of the same curve, the Fig. 3 shows that the complete curve may sometimes undergo a looping; see for instance the curves $(j,i) = \{(1,1),(1,2),(2,1),(2,2),(3,1),(4,1)\}$. For the rest of the cases this looping does not manifest (see the curves $(j,i) = \{(3,2),(4,2)\}$). In those cases with looping, the critical curves seem to enclose two overdamped regions: in one of them the values of ζ verify $\zeta_{Uj}^{(i)}(\nu) \le \zeta \le \zeta_{Lj}^{(i)}(\nu)$ and, in the other one, $\zeta_{Lj}^{(i)}(\nu) \le \zeta \le \zeta_{Uj}^{(i)}(\nu)$. The approximate overdamped region associated to this curve will fulfill this latter condition. In those curves without looping, there exists only one region verifying $\zeta_{Lj}^{(i)}(\nu) \le \zeta \le \zeta_{Uj}^{(i)}(\nu)$, thus there is no place for ambiguity in them about the overdamped region.

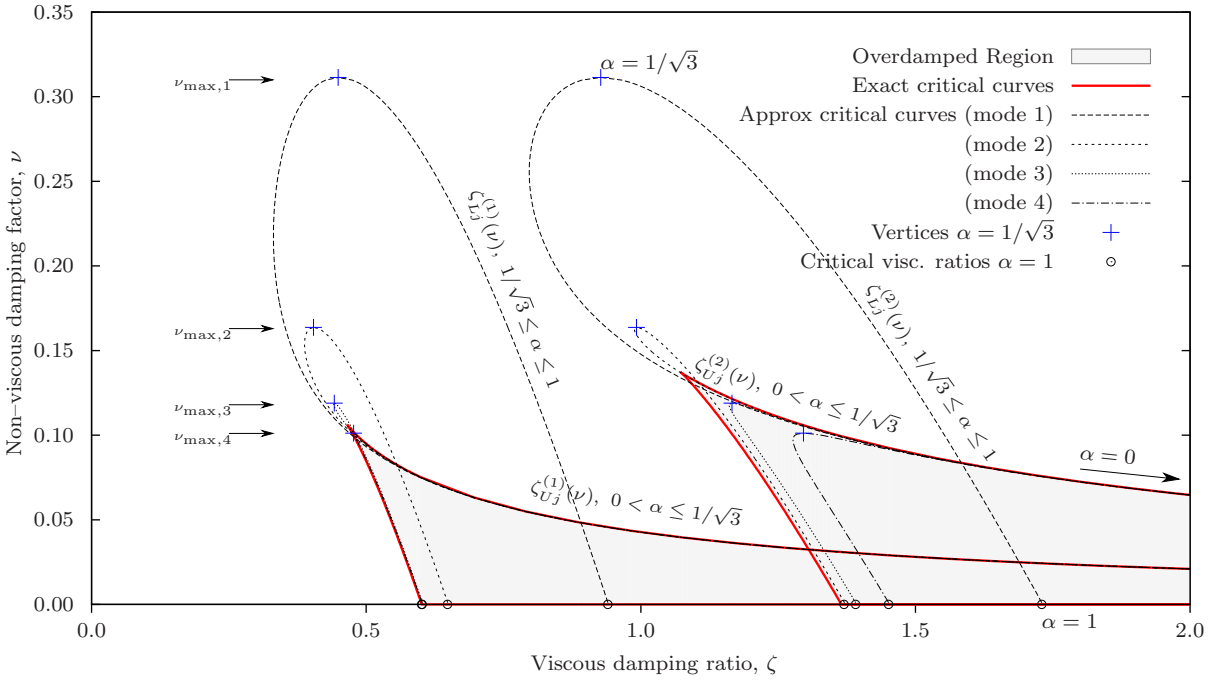

Figure 3: Example 1: Critical damping curves and the corresponding enclosing overdamped regions for the four degrees-of-freedom system.

As aforementioned, there is also an alternative way to depict the critical curves, considered them in parametric form. From Eq. (58), the nonviscous factor $\nu = \omega_r/\mu$ can be expressed as

$$\nu_{cj}(\alpha) = \frac{\omega_r}{\mu} = \frac{\omega_r}{2\omega_j}\,\alpha\,\left(1-\alpha^2\right) \tag{72}$$

where the meaning of the parameter α is directly related to the real eigenvalue through $s_{cj} = -\omega_j/\alpha$ and is defined in the range $0 < \alpha \le 1$. Since both $\nu_{cj}(\alpha)$ and $s_{cj}(\alpha)$ can be then expressed as function of α, the critical damping ratios $\zeta = c/2m\omega_r$ arise from the solution of the equation

$$\det\left[\mathbf{A}_j(\alpha)/2m\omega_r - \zeta\,\mathbf{J}\right] = 0 \tag{73}$$

where the matrix $\mathbf{A}_j(\alpha)$ has been defined in Eq. (61) and

$$\mathbf{J} = \mathbf{C}/c = \begin{bmatrix} 0 & 0 & 0 & 0 \\ 0 & 1 & -1 & 0 \\ 0 & -1 & 2 & -1 \\ 0 & 0 & -1 & 1 \end{bmatrix} \tag{74}$$

The Eq. (73) is equivalent to solve the linear eigenvalue problem in ζ

$$\left[\mathbf{A}_j(\alpha)/2m\omega_r - \zeta\,\mathbf{J}\right]\mathbf{u} = \mathbf{0} \tag{75}$$

for each value of α within $0 < \alpha \le 1$, something that is computationally much more efficient for lager systems. Since $\mathrm{rank}(\mathbf{J}) = 2$, then two critical curves can be determined as the sets of points

$$\left\{\left(\nu_{cj}(\alpha), \zeta_j^{(1)}(\alpha)\right) \in \mathbb{R}^2 : 0 < \alpha \le 1\right\}\ ,\quad \left\{\left(\nu_{cj}(\alpha), \zeta_j^{(2)}(\alpha)\right) \in \mathbb{R}^2 : 0 < \alpha \le 1\right\} \tag{76}$$

The notation adopted for these two curves associated to the mode j is not arbitrary because, actually, the curve $\left(\nu_{cj}(\alpha), \zeta_j^{(i)}(\alpha)\right)$ in parametric form, follows the same graph as the union of the curves $(\nu, \zeta_{Lj}^{(i)}(\nu))$ and $(\nu, \zeta_{Uj}^{(i)}(\nu))$. The point corresponding to $\alpha = 1/\sqrt{3}$ delimits both branches and also coincides with the location where ν does not change, that is $\partial\nu_{cj}/\partial\alpha = 0$ holds at $\alpha = 1/\sqrt{3}$. Thus, a set of local maximums for each mode can be found after plugging $\alpha = 1/\sqrt{3}$ into Eq. (72), values which have been listed in Table 2 and plotted in Fig. 3. The ends of each curve are associated with the limits of the interval $\alpha \in (0, 1]$. As

	Mode 1	Mode 2	Mode 3	Mode 4
$\nu_{\max,j} = \omega_r/3\sqrt{3}\omega_j$	0.31139	0.16370	0.11894	0.10117

Table 2: Example 1: Maximum values of the nonviscous factor $\nu_{\max,j}$ for each mode.

the α parameter gets closer to the lower bound $\alpha = 0$, the critical eigenvalue tends to $s_{cj}(0) \to -\infty$. The points (ζ, ν) are then located along the asymptotic branches (see Fig. 3). On the contrary, the upper bound $\alpha = 1$ corresponds to $s_{cj} = -\omega_j$ and $\nu_{cj}(1) = 0$, distinctive of a viscous system. The intersection of the critical curves with the ζ-axis (represented in Fig. 3 with circles) depict the critical viscous damping relationships.

In this example the proposed overdamped regions associated to the critical curves $\{(\nu_{cj}(\alpha), \zeta_j^{(1)}(\alpha)), 1 \leq j \leq 4\}$ are enveloped by that one of the mode $j = 2$. Similarly, those regions associated to $\{(\nu_{cj}(\alpha), \zeta_j^{(2)}(\alpha)), 1 \leq j \leq 4\}$ lie inside the overdamped region of the mode $j = 4$. Since the overdamped region of the system results from the union of simple modal regions, only those critical curves that envelop the rest can be left. By doing this for the current example, it arises the overdamped region in Fig. 4(a). This figure shows that the proposed critical curves depict a great accuracy respect to the exact ones along the entire range $0 < \alpha \leq 1$.

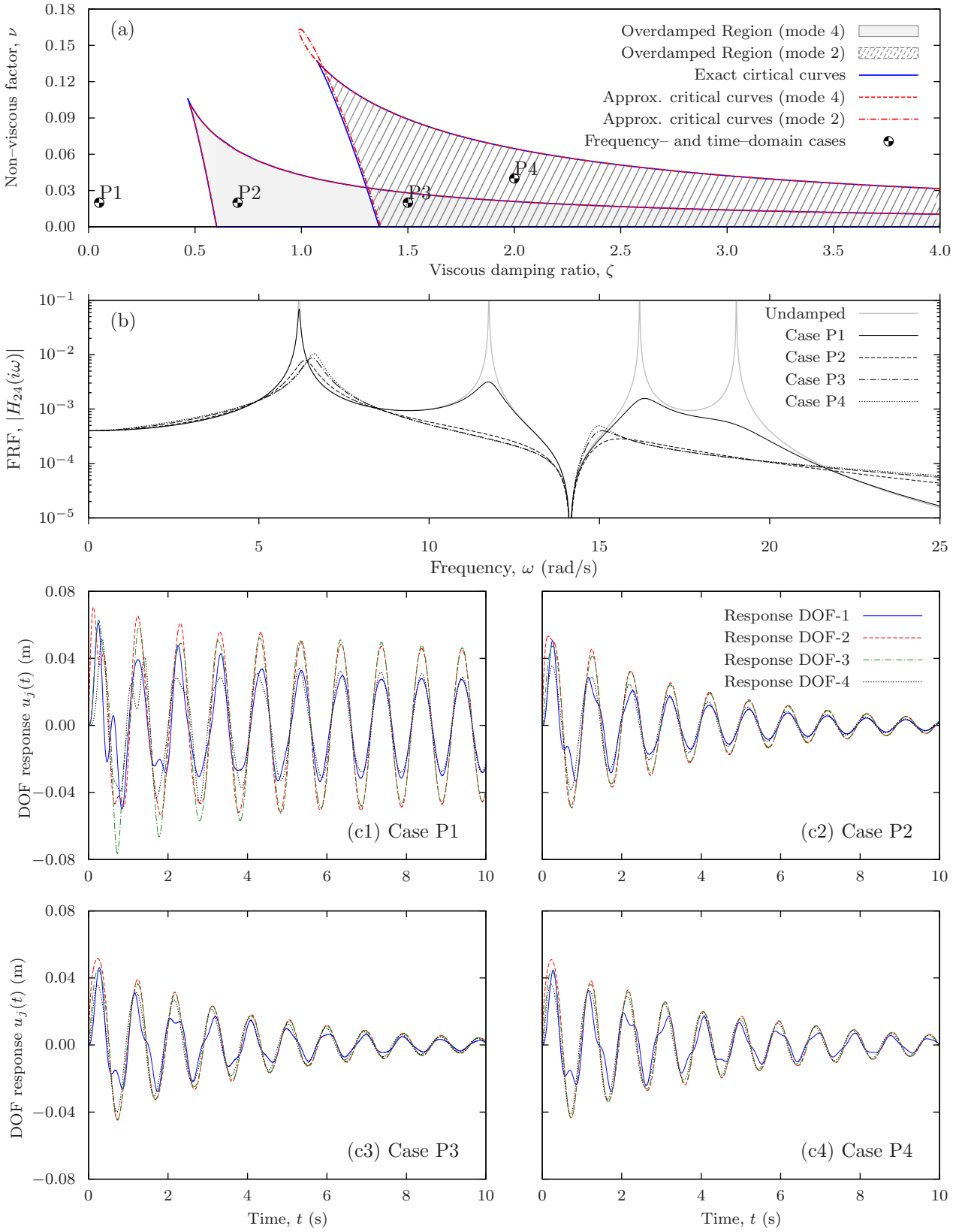

Figure 4: Response plots for Example 1. (a): Representation of the maximum overdamped regions for the 4-dof discrete system, for modes 2nd and 4th and four cases of damping parameters. (b): Frequency Response Function for the four damping cases, P1 to P4. (c1) to (c4): Time domain response of degrees of freedom for cases P1 to P4 respectively

As expected, in those zones with more discrepancies between approximate and exact curves (see for instance the branch $\zeta_{L2}^{(2)}(\nu)$), the proposed approach lies always inside the exact overdamped region, showing the conservative character of the proposed method. This behavior can be generalized since it is a consequence of the approximate nature of the method. Indeed, if the approach gave exact eigensolutions, these ones would be associated to the maximum region in the plane (ζ, ν) [7].

As performed for the single dof example, it is interesting to show some simulations of the system for different damping cases. The Fig. 4(a) will be used to place in the parametric domain the four considered cases: P1, P2, P3 and P4. Each combination of parameters allows to construct with precision the damping model and therefore the response in both frequency- and time-domain can be determined. In Fig. 4(b) the frequency response function (FRF) $H_{24}(\omega)$ has been plotted in absolute value, including the undamped case. This latter clearly shows the location of the natural frequencies before the damping perturbation. In the case P1, although all modes still present oscillatory behavior, the amplitudes of 2nd, 3rd and 4th mode have been significantly reduced as a consequence of damping. Case P2 lies within the overdamped region of the 4th mode, as observed in Fig. 4(a). From the FRF plot, it can not be clarified which mode is now critical since modal peaks of both 2nd and 4th seem to have disappeared. FRF curves do not present relevant changes from case P2 to P4 except for the fact that case P4 seem to be slightly less damped than P2 and P3, probably because of a higher value of the nonviscous factor ν (associated to a lower value of the relaxation parameter μ).

Time-domain simulations have been carried out using the state-space approach associated to the unforced system [16] under the initial conditions $\mathbf{u}(0) = \mathbf{0}$, $\dot{\mathbf{u}}(0) = (0, 1, 0, 0)$. Response curves of the four degrees fo freedom have been represented in Figs. 4(c1) to (c4) for each one of the aforementioned damping cases (P1 to P4) respectively. For the case P1, the system has four modes with oscillatory nature whose effect in the response can be noticed within the first instants of time in Figs. 4(c1). Since 2nd to 4th modes are significantly more damped than the first one, see Fig. 4(b), after some seconds the system finally responds as if it were oscillating in the first mode. For the case P2, the 2nd mode becomes completely overdamped and the 3rd and 4th mode depicts a noticeable reduction of the modal amplitude and a increasing of the corresponding modal damping, compared to case P1. Hence, their effect on the time-domain response disappear even before than that of the case P1 (see Fig. 4(c2)). In cases P3 and P4 the amplitude of the 3rd mode is slightly higher and its damping lower than those of case P2. Therefore, its associated time-domain plots show this fact in Figs. 4(c3) and (c4), where, indeed, the outcome of two frequencies can be observed (1st and 3rd modes) along the entire simulation time.

6. Numerical example 2: Continuous system

In this example the proposed method is validated for larger systems with many degrees of freedom. For that purpose, a continuous cantilever beam of length $l = 5$ m with three local viscoelastic supports is considered (see Fig. 5). The beam is modeled using $n_e = 12$ two-nodes Euler-Bernoulli finite elements. Each node has three degrees of freedom (two displacements and rotation); thus the structural model has a total number of $n = 36$ degrees of freedom. The assumed material is steel with Young modulus $E = 210$ GPa and density $\rho = 7.85$ t/m^3. The cross section is constant with a flexural stiffness of $EI = 224$ kNm^2 and a mass per unit of length of $\rho A = 0.0628$ t/m. The nonviscous dissipative behavior is introduced throughout three viscoelastic constraints, located at sections $l/3$, $2l/3$ and l affecting to the vertical displacements. Each link is formed by a linear spring together with a nonviscous exponential damping function. The stiffness of the springs are $k_1 = k_2 = 3.58$ kN/m and $k_3 = 7.17$ kN/m. According to the assumed hypothesis in this paper, the three associated exponential kernels are controled under the same relaxation parameter μ. Hence,

$$\begin{aligned} \mathcal{G}_1(t) &= \mu\, c_1\, e^{-\mu t} \\ \mathcal{G}_2(t) &= \mu\, c_2\, e^{-\mu t} \\ \mathcal{G}_3(t) &= \mu\, c_3\, e^{-\mu t} \end{aligned} \tag{77}$$

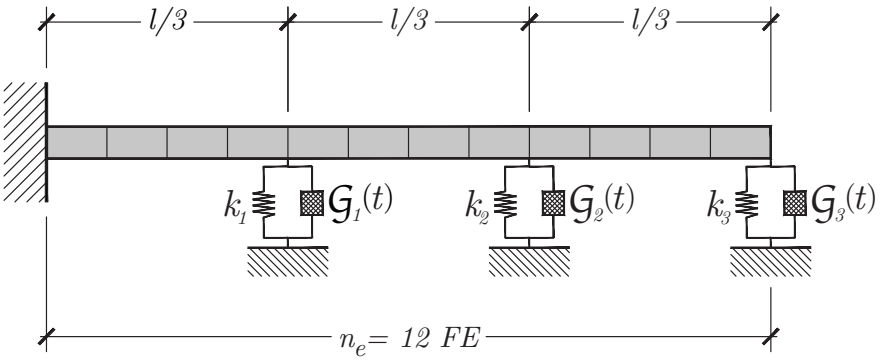

Figure 5: Example 2: A continuous beam with 12 finite element, 36 degrees of freedom and three viscoelastic supports.

Thus, the damping matrix yields $\boldsymbol{\mathcal{G}}(t) = \mu\, e^{-\mu t}\, \mathbf{C}$, where $\mathbf{C} = [C_{ij}]$ is the viscous matrix with zeros in all entries except those ones associated to the dampers' degrees of freedom; in particular $C_{11,11} = c_1,\ C_{23,23} = c_2,\ C_{35,35} = c_3$. For this example the three viscous coefficients will be assigned as follows $c_1 = 2c_r,\ c_2 = c_r,\ c_3 = c_r$, where c_r is a reference parameter. As common practice, instead of c_r, it is always preferable to introduce the dimensionless viscous damping ratio, ζ, defined as $\zeta = c_r/2m_r\omega_r$, where $m_r = 0.314$ t is the total mass of the beam and $\omega_r = \sqrt{EI/ml^3} = 2.3889$ rad/s is the reference frequency. In addition, let $\nu = \omega_r/\mu$ denote the dimensionless nonviscous parameter.

For large systems it results suitable to draw the critical curves using the parametric approach based on the already defined parameter α. In this numerical example the rank of the damping matrix is $p = \operatorname{rank}\mathbf{C} = 3$, hence a total number of $n \times p = 36 \times 3 = 108$ critical curves can be plotted. Each curve is defined in parametric form using the parameter α, which sweeps out the interval $0 < \alpha \leq 1$. For each $\alpha \in (0, 1]$ and for each mode $1 \leq j \leq n$, three values of the damping ratio are found solving the following linear eigenvalue system in ζ.

$$[\mathbf{A}_j(\alpha)/2m_r\omega_r - \zeta\, \mathbf{J}]\ \mathbf{u} = \mathbf{0} \tag{78}$$

where $\mathbf{J} = \mathbf{C}/c$ and $\mathbf{A}_j(\alpha)$ has already been presented in Eq. (61). The results have been plotted in the Fig. 6 covering a domain of the damping parameters $0 \leq \zeta \leq 30$, $0 \leq \nu \leq 0.1$. The three curves associated to each mode, reach the maximum $\nu_{\max,j} = 1/3\sqrt{3}\omega_j$. It is clear then that these maximum values decrease as the mode increases, due to the presence of the associated natural frequency in the denominator. Also in the same figure, a shaded region representing the exact overdamped region has also been represented. The determination of this region has been carried out solving the eigenvalue problem (3) for each pair (ζ, ν) defined on a grid fine enough within the aforementioned limits. As known [22, 23], the number of nonviscous eigenvalues in a exponentially damped system is equal to $p = \operatorname{rank}(\mathbf{C})$. If, after evaluating the set of eigenvalues for a certain pair (ζ, ν), a higher number of real eigenvalues is found, it means that this pair lies inside the overdamped region.

Although this system is different in nature of that one of the previous example, similarities between their critical curves can be found. Thus, all of them have a point in common at $(\zeta, \nu) = (+\infty, 0)$, corresponding to $\alpha \to 0$. From this point (at the infinite) up to the maximum value at $\nu_{\max,j}$, the parameter α varies from $\alpha = 0$ up to $\alpha = 1/\sqrt{3}$, being this branch that one corresponding to the set of points of the form $(\nu, \zeta_{Uj}^{(i)}(\nu))$. If we keep evaluating the parameter α in the interval $1/\sqrt{3} \leq \alpha \leq 1$, it results the branch $(\nu, \zeta_{Lj}^{(i)}(\nu))$. The last point (for $\alpha = 1$) corresponds to the critical purely viscous damping ratio. As previously pointed out, in some cases the proposed critical curves can present a looping along their path in the parametric domain, as for instance two of those curves associated to the first mode or the third one of the second mode. In these

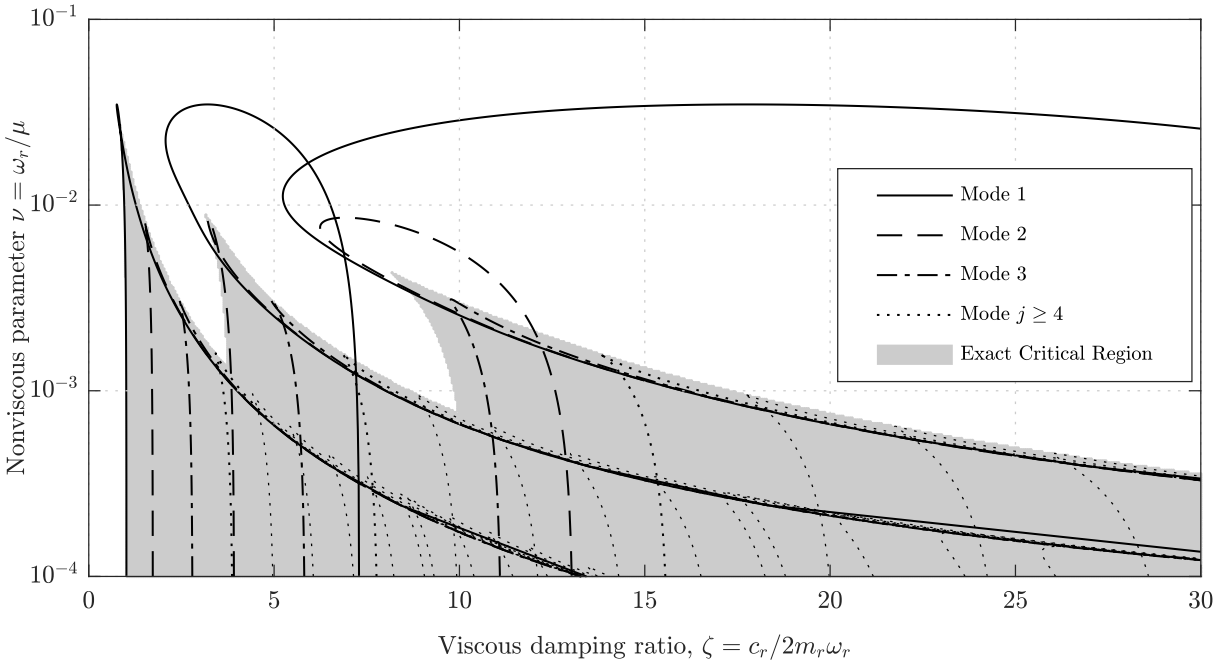

Figure 6: Example 2: Approximate critical curves for the twelve first modes. One can observe three overdamped regions corresponds because the rank of the damping matrix is $p = \text{rank}(\mathbf{C}) = 3$. Critical curves of the fourth mode and those higher ones are approximately surrounded by those curves associated to lower modes

cases, the region verifying $\zeta_{Lj}^{(i)} \leq \zeta \leq \zeta_{Uj}^{(i)}$ represents the proposed overdamped area. Moreover, as predicted, the so formed overdamped region always lie inside the exact one, as shown in the Fig. 6.

In this example, the overdamped region seems to depic the intersection of three subregions corresponding to the critical damping associated with the first, second and third modes. At first sight, the approximate critical curve for the first mode has better fit respect to the exact region than that of the second mode. In turn, the latter has visibly less errors than the critical curve of the third mode. Therefore, it seems that the quality of the proposed region gets worse as we move to the right in the (ζ, ν) plane. This, although more slightly, has also been visualized in the previous example, where the critical curves associated to the 2nd mode (visibly located rightwards) also depicted higher discrepancies than those of the 4th mode.

In view of the results, it seems that the critical behavior is dominated by the three first modes and the proposed overdamped region is almost totally enclosed by just three critical curves associated to these modes. In general, it is expected that the distribution of the dissipative devices along certain structure will affect to a limited number of modes whose critical curves will envelope to the rest. Thus, it should not be necessary to compute the whole set of critical curves (in number equal to $n \times \text{rank}\,\mathbf{C} = 108$ in this example), but only up to certain mode, from which every new critical curve will lie inside the already drawn region. Taking this into account, the computational cost of determining the approximate overdamped region can be significantly reduced.

7. Conclusions

In this paper, nonviscously damped systems under Biot's exponential models are under consideration. Nonviscous or viscoelastic vibrating structures present dissipative forces depending on the past history of the velocity response via convolution integrals over hereditary kernels. The oscillatory nature of the response

(associated to complex eigenvalues) is directly conditioned by the damping parameters controlling the dissipative behavior. For certain combination of these parameters, the oscillatory nature of the response can be lost and become non-oscillatory (negative real eigenvalues). It is said then that some (or all) modes are overdamped. Within the domain of the damping parameters, the boundaries between oscillatory and non–oscillatory induced motion are named critical surfaces (critical curves if only two parameters are considered).

The determination of the critical surfaces of a nonvisously damped system can be addressed eliminating the Laplace parameter s from the determinant of the system $\det[\mathbf{D}(s)] = 0$ and from its derivative $\partial/\partial s(\det[\mathbf{D}(s)]) = 0$. When the size of the system increases, the computation of closed-forms for these determinants becomes computationally inefficient. In this paper a new numerical method to the approximation of critical curves for nonviscously damped systems based on one exponential hereditary kernel is proposed. Using functional principles and the implicit function theorem, it is proved that the critical curves can be approximated eliminating the parameter s from $\det[\mathbf{D}(s)] = 0$ and from $\det[\mathbf{D}'(s)] = 0$. It turns out that the resulting critical eigenvalues are close related to those of the single-degree-of-freedom nonviscous oscillator; in fact, they are the roots of a third order polynomial, named *critical modal equation*. It is proved that for each mode of the undamped system, a set of $p = \text{rank}(\mathbf{C})$ approximate critical curves can be derived.

The proposed numerical approach is first validated with the overdamped region for a single degree-of-freedom system (available from the literature). In addition, two numerical examples for multiple degrees of freedom are also developed. The first one is focused on a discrete system formed by 4 masses attached with linear rigidities together with two nonviscous dampers. The obtained critical curves found with the proposed method have been compared with the exact one, achieving very good agreement between approximated and exact overdamped regions. The second example is specially constructed to validate the proposed method for larger systems, involving continuous structures and subjected to discrete nonviscous dampers. As predicted by the theory, the overdamped region is enclosed by set of $n \times p$ critical curves (where n is the number of degrees of freedom). However, in practice, only a few are needed to cover almost all overdamped region. Satisfactory agreements between the actual and the exact results were obtained. The outcomes of this work open new ways to study critical surfaces in nonviscous systems. The challenge for future works is to extend the methodology for even more general systems with multiple degrees of freedom involving multiple exponential kernels.

References

[1] S. Adhikari, Dynamics of non-viscously damped linear systems, Journal of Engineering Mechanics 128 (3) (2002) 328–339.
[2] D. Golla, P. Hughes, Dynamics of viscoelastic structures - a time-domain, finite-element formulation, Journal of Applied Mechanics-Transactions of the ASME 52 (4) (1985) 897–906.
[3] M. Lázaro, J. L. Pérez-Aparicio, Characterization of real eigenvalues in linear viscoelastic oscillators and the non-viscous set, Journal of Applied Mechanics (Transactions of ASME) 81 (2) (2014) Art. 021016–(14pp).
[4] M. Lázaro, Nonviscous modes of nonproportionally damped viscoelastic systems, Journal of Applied Mechanics (Transactions of ASME) 82 (12) (2015) Art. 121011 (9 pp).
[5] D. Beskos, B. Boley, Critical damping in linear discrete dynamic-systems, Journal of Applied Mechanics-Transactions of The ASME 47 (3) (1980) 627–630.
[6] M. Lázaro, Critical damping in non-viscously damped linear systems, Applied Mathematical Modelling (In Press, 2019-Vol. 65)doi:https://doi.org10.1016/j.apm.2018.09.011.
[7] R. Duffin, A minimax theory for overdamped networks, Journal of Rational Mechanics and Analysis 4 (2) (1955) 221–233.
[8] D. Nicholson, Eigenvalue bounds for damped linear systems, Mechanics Research Communications 5 (3) (1978) 147–152.
[9] P. Muller, Oscillatory damped linear-systems, Mechanics Research Communications 6 (2) (1979) 81–85.
[10] D. Inman, A. Andry, Some results on the nature of eigenvalues of discrete damped linear-systems, Journal of Applied Mechanics-Transactions of The ASME 47 (4) (1980) 927–930.
[11] L. Barkwell, P. Lancaster, Overdamped and Gyroscopic Vibrating Systems, Journal of Applied Mechanics-Transactions of The ASME 59 (1) (1992) 176–181.
[12] A. Bhaskar, Criticality of damping in multi-degree-of-freedom systems, Journal of Applied Mechanics, Transactions ASME 64 (2) (1997) 387–393, cited By 7.
[13] A. Muravyov, Forced vibration responses of viscoelastic structure, Journal of Sound and Vibration 218 (5) (1998) 892–907.
[14] S. Adhikari, Qualitative dynamic characteristics of a non-viscously damped oscillator, Proceedings of the Royal Society A-Mathematical Physical and Engineering Sciences 461 (2059) (2005) 2269–2288.

[15] P. Muller, Are the eigensolutions of a l-d.o.f. system with viscoelastic damping oscillatory or not?, Journal of Sound and Vibration 285 (1-2) (2005) 501–509.
[16] A. Muravyov, S. Hutton, Free vibration response characteristics of a simple elasto-hereditary system, Journal of Vibration and Acoustics-Transactions of the ASME 120 (2) (1998) 628–632.
[17] S. Papargyri-Beskou, D. Beskos, On critical viscous damping determination in linear discrete dynamic systems, Acta Mechanica 153 (1-2) (2002) 33–45.
[18] C. Bert, Material Damping - Introductory Review Of Mathematical-models, Measures And Experimental Techniques, Journal of Sound and Vibration 29 (2) (1973) 129–153.
[19] A. Muravyov, Analytical solutions in the time domain for vibration problems of discrete viscoelastic systems, Journal of Sound and Vibration 199 (2) (1997) 337–348.
[20] M. Biot, Theory of stress-strain relations in anisotropic viscoelasticity and relaxation phenomena, Journal Of Applied Physics 25 (11) (1954) 1385–1391.
[21] M. Abramowitz, I. A. Stegun, Handbook of mathematical functions, with formulas, graphs and mathematical tables, Dover Publications Inc., 1965.
[22] N. Wagner, S. Adhikari, Symmetric state-space method for a class of nonviscously damped systems, AIAA Journal 41 (5) (2003) 951–956.
[23] S. Adhikari, N. Wagner, Analysis of asymmetric nonviscously damped linear dynamic systems, Journal of Applied Mechanics (Transactions of ASME) 70 (6) (2003) 885–893.